Fate of sulfamethoxazole in groundwater: conceptualizing and modeling metabolite formation under different redox conditions

Paula Rodríguez-Escales*, Xavier Sanchez-Vila

Hydrogeology Group (UPC-CSIC), Dept. of Civil and Environmental Engineering. Universitat Politècnica de Catalunya, Jordi Girona 1-3, 08034 Barcelona, Spain

***Corresponding author:** paula.rodriguez.escales@upc.edu

ABSTRACT

Degradation of emerging organic compounds in saturated porous media is usually postulated as following simple low-order models. This is a strongly oversimplified, and in some cases plainly incorrect model, that does not consider the fate of the different metabolites. Furthermore, it does not account for the reversibility in the reaction observed in a few emerging organic compounds, where the parent is recovered from the metabolite. One such compound is the antibiotic sulfamethoxazole (SMX). In this paper, we first compile existing experimental data to formulate a complete model for the degradation of SMX in aquifers subject to varying redox conditions, ranging from aerobic to iron reducing. SMX degrades reversibly or irreversibly to a number of metabolites that are specific of the redox state. Reactions are in all cases biologically mediated. We then propose a mathematical model that reproduces the full fate of dissolved SMX subject to anaerobic conditions and that can be used as a first step in emerging compound degradation modeling efforts. The model presented is tested against the results of the batch experiments of Barbieri et al. (2012) and Nödler et al. (2012) displaying a non-monotonic concentration of SMX as a function of time under denitrification conditions, as well as those of Mohatt et al. (2011), under iron reducing conditions.

Keywords

Sulfamethoxazole, denitrification, oxidation-reduction, co-metabolism, metabolites, modeling

1 Introduction

The presence of pharmaceutical compounds in aquatic environments has been frequently addressed in recent years, and it is the topic of numerous review articles (Gavrilescu et al. 2015, Schwarzenbach et al. 2006). The discharge of antibiotics into the environment has become a major concern, as this group of pharmaceuticals is not only prone to directly influencing microbial communities (Fent et al. 2006, Yan et al. 2013), but also because of the risk of worldwide dispersal of antibiotic-resistant bacterial genes (Szczepanowski et al. 2009). Antibiotics may enter the environmental system via wastewater or else as wastewater treatment plant (WWTP) effluents, diffusive agricultural input (Ijemba 2002), or landfill discharge (Heberer 2002), and they can be found in different environmental compartments such as surface and subsurface water bodies, sediments, and soils.

Sulfamethoxazole (SMX) is a polar sulfonamide antibiotic, and the most widely detected antibiotic in aquatic environments (Gao et al. 2014). SMX mainly enters wastewater via human excretion either unmodified or as its human-metabolized transformation products, N-acetyl-SMX or N-SMX-glucuronide (Göbel et al. 2005). Both transformation products are easily cleaved back to the SMX parent compound (Göbel et al. 2005). Since SMX is not completely degraded in wastewater treatment plants, it is found in minute concentrations in the WWTP water effluents, eventually reaching soils and surface or subsurface water bodies. Actually, it has been found in concentrations up to 0.47 µg/L in aquifers and 0.48 µg/L in surface waters (Hirsch et al. 1999). SMX has a very low adsorptivity to most soils (Henzler et al. 2014, Schaffer et al. 2015). Thus, it is postulated that sorption into aquifer sediments is usually negligible, so that the observed reduction of concentrations of SMX in the environmental compartments is mainly due to degradation.

In general, the literature on SMX degradation in both WWTPs and natural aqueous environments is marked by inconsistent results. This is supposedly because elimination amounts and rates depend on various environmental factors such as *in situ* redox potential, available nutrients, soil characteristics, seasonal temperature, microbial adaptation, and light variations (Müller et al. 2013), all such factors being site-dependent and temporally variable.

Based on field observations and laboratory experiments, it is postulated that degradation of SMX is biologically mediated and occurs preferentially under strictly anaerobic conditions (Banzhaf et al. 2012, Grünheid et al. 2005, Heberer et al. 2008, Schaffer et al. 2015, Valhondo et al. 2015). Some lab experiments reported the fate of SMX for particular redox conditions such as denitrification (e.g., Barbieri et al. 2012, Nödler et al. 2012) or iron reducing conditions (e.g., Mohatt et al., 2011). Nevertheless, aerobic degradation of SMX has also been observed in aerobic environments such as activated sludge (Baumgarten et al. 2011, Drillia et al. 2005, Gauthier et al. 2010, Reis et al. 2014).

Besides biological processes, abiotic SMX elimination has also been reported. For example, chemical oxidation was found to be an effective degradation process by using persulfate in the presence of ferrous iron oxidizing to ferric iron (Ji et al. 2014). The complementary mechanism was described in Mohatt et al. (2011), where abiotic degradation was enhanced by the biological reduction of ferric iron into ferrous iron.

Only in experiments performed under either aerobic conditions sustained for large times (Müller et al. 2013, Reis et al. 2014) or in anaerobic iron reducing conditions (Mohatt et al. 2011), the irreversible breakage of the SMX molecule was observed. Contrarily, the metabolites observed during denitrification conditions resulted from the substitution of the primary amine of SMX, forming either 4-nitro-SMX or else desamino-SMX (Barbieri et al. 2012, Nödler et al. 2012). In these last two papers, the authors reported that metabolites were not stable, meaning that when the denitrification process was over they were retransformed into the parent compound (see also Banzhaf et al. 2012).

Despite all the existing literature dealing with the fate of SMX under different redox conditions, there is little work postulating the processes taking place at the molecular scale, proposing closed-form expression for reaction rates, and reproducing the experimental observations of SMX fate through mathematical modeling. According to Henzler et al. (2014), this assertion is also valid for a large number of emerging organic compounds (EOCs). Most of the published works assume that degradation can be explained by (apparent) first-order degradation rates for all EOCs in a given cocktail (Henzler et al. 2014, Nham et al. 2015, Schaffer et al. 2015). Only few studies have investigated quantitatively the actual processes driven by varying redox conditions over degradation rates of EOCs (Greskowiak et al. 2006, Liu et al. 2013). Moreover, this simplified approach, based on first-order reactions, accounts only for the presence of irreversible reactions, contradicting a number of experiments where reversibility of the transformation processes has been observed (Barbieri et al. 2012, Stadler et al. 2015). While it is obvious that each antibiotic displays an individual, non-generalizable degradation behavior, it is also true that understanding one of them will open the door to analyze in the future the fate of a cocktail of antibiotics (and their metabolites), including also potential synergies.

Considering all of this, the objective of this work was to develop a conceptualization of the molecular mechanisms of degradation of the sulfamethoxazole molecule under different redox conditions ranging from aerobic to iron-reducing conditions, and a mathematical model capable of reproducing these mechanisms, with the overall aim of tracing the metabolite formation from different degradation pathways. To our knowledge, this is the first work which integrates all known processes on the degradation pathways of sulfamethoxazole as well as its metabolites in groundwater and under different redox conditions in a consistent mathematical framework that is able to describe various experimental data sets. To illustrate the conceptual and mathematical work, we model and interpret three published experiments, two of them

103 performed under nitrate reducing conditions (Barbieri et al., 2012; Nödler et al., 2012), and
104 one under iron reducing ones (Mohatt et al., 2011).

105 ## 2 Methods

106 ### 2.1 Observations and conceptualization of the molecular mechanisms

107 The literature provides information regarding degradation of SMX only under aerobic and
108 partially under anaerobic (nitrate and iron reduction) conditions. Although in Mohatt et al.
109 (2011) SMX degradation under sulfate reduction condition was observed, to our knowledge,
110 no experimental information is available describing such process, and thus no metabolites
111 have been observed. So, in this work we conceptualize the SMX degradation for aerobic
112 conditions, denitrification, and iron reducing conditions.

113 #### 2.1.1 SMX behavior under aerobic conditions

114 Aerobic degradation of SMX has been mostly studied in the context of WWTPs and surface
115 water bodies, and it is not expected to be a significant process in groundwater bodies due to
116 their generally low oxygen concentrations. Degradation has mostly been observed for large
117 SMX concentrations (WWTP range) and with acclimated biomass in activated sludge systems
118 (Müller et al. 2013, Reis et al. 2014). SMX degradation was observed either via direct
119 metabolism or else via co-metabolism (Gauthier et al., 2010; Reis et al., 2014; Drillia et al.,
120 2005); in the latter case, degradation rates were generally comparably larger. Additionally, one
121 study reported aerobic degradation of SMX in a column experiment supplied with surface
122 water (Baumgarten et al. 2011). The degradation was linked to large adaptation times, around
123 1 year for the degradation at the lowest concentration of SMX (0.25 µg/L) and 3-12 months for
124 the highest reported one (1.4 µg/L).

125 The most frequent metabolite produced under aerobic conditions was 3-amino-5-
126 methylisoxazole (Müller et al. 2013, Reis et al. 2014). This metabolite represents an irreversible
127 breakage of the SMX molecule, more precisely of the sulfonamide radical, in concordance with

the aerobic degradation pathway first predicted by Gao et al. (2010) (Figure 1). This pathway would facilitate the complete mineralization of 4-aminobenzolsulfonate (a by-product of the reaction), as this compound could also be degraded under aerobic conditions (Gao et al. 2010).

According to different authors (Baumgarten et al. 2011, Gauthier et al. 2010, Reis et al. 2014), aerobic degradation can be modeled as first-order kinetics. Table 1 shows a review of the apparent half-lives for SMX degradation compiled from experiments available in the literature. It is noticeable that all half-live values were determined whenever biomass was completely acclimated; this would indicate that in more general systems, with no acclimated biomass, real half-lives (if at all existing) would be larger.

2.1.2 SMX behavior under nitrate reducing conditions

As already presented in the introduction, SMX degradation under nitrate reducing conditions has been widely reported. Because of the controlled conditions of the experiments and metabolite monitoring we have focused our analysis in the works of Barbieri et al., 2012 (from now on BAR) and Nödler et al., 2012 (denoted NDL in the sequel).

2.1.2.1 Observations and possible inference

The BAR and NDL experiments were developed under identical experimental conditions, involving sets of microcosms containing natural sediments, synthetic water and SMX (injected in a cocktail of EOCs). They included a set of biotic and abiotic series by duplicate to separate biodegradation (both biotic mineralization and transformation included here) from sorption or other abiotic processes. The experiments were performed inside a glove box under Argon atmosphere and into 0.3 L glass bottles running for 21 days in the BAR experiment and 90 days for NDL. Bottles were filled with 0.24 L of water with the chemical signature provided in Table 2 and 120 g of air-dried and homogenized quaternary alluvial sediments composed by quartz, calcite, albine, dolomite, clonochlore and illite in different proportions. The organic carbon and the nitrogen present in the sediment were lower than 0.2% in mass. Mn and Fe (III) associated

153 to oxide-hydroxides and oxides were 0.007% for Mn and 0.584% for total Iron. Denitrification
154 conditions were stimulated by adding easily degradable organic compounds (sodium acetate
155 and methanol) to act as electron donors. Additional information and analytical details can be
156 found in Barbieri et al. (2012) and in Barbieri et al. (2011). Concurrently, a set of abiotic
157 experiments were performed with an identical full setup except that a small concentration of
158 $HgCl_2$ was added to the solution in order to inhibit biological activity.

159 The results of the biotic experiments showed a decrease in time of nitrate and organic
160 carbon after lag phases of 1.8 and 3 d in the BAR and NDL experiments, respectively (Figures
161 2a and 2d). The lag phase was attributed to an adaption period for the denitrifying bacteria. A
162 transient accumulation of nitrite taking place simultaneously with a decrease in nitrate was
163 observed in both experiments, indicating partial denitrification. After 10 days, nitrate and
164 nitrite were completely depleted in the BAR experiment. After that (between 10 and 21 days) a
165 small production of Mn^{+2} and Fe^{+2} was observed indicating a transition towards stronger
166 reducing conditions (lower Eh). On the other hand, in the NDL experiment denitrification was
167 active even after 90 days, with remaining concentrations of nitrate and nitrite of 3.5 and 0.16
168 mM, respectively, suggesting incomplete denitrification by the end of the experiment.

169 Almost full depletion of SMX was observed during the period corresponding to transient
170 accumulation of nitrite in both experiments (Figures 2b, 2e). During this time, the metabolite
171 4-nitro-SMX was detected and quantified in both experiments, whereas a second metabolite,
172 desamino-SMX, was also detected in NDL experiment (it was not monitored in BAR). After
173 denitrification was over (BAR) or close to being complete (NDL), the two metabolites were
174 virtually depleted in the system, while SMX reappeared, reaching concentration values of the
175 same order than the initial injected ones. At this point it is relevant to state that the NDL
176 experiment involved an initial concentration of SMX 1000 times larger than that of BAR (recall
177 Table 2), indicating that the process was not an artifact attributable to high or low input
178 concentrations.

179 Regarding the abiotic experiments, the concentration of SMX remained constant during
180 all the duration of the experiment indicating that SMX depletion in the biotic experiments was
181 driven by biological activity (Figures 2a-f).

182 Concerning the mass balance of SMX compounds, the BAR experiment showed a gap
183 during the denitrification phase, and by the end of the experiment the concentration of SMX
184 was about 75% of the initial value (Figure 2c). On the other hand, the mass balance in NDL had
185 a sudden decay of about 45% at the first sampling point (day 5) and from then on it remained
186 approximately constant until the end (day 90) of the experiment (Figure 2f). As experimental
187 conditions were similar in the two experiments, we assumed that the gap observed in the
188 mass balance of BAR could represent the formation of the desamino-SMX metabolite (not
189 measured). Thus, it seemed that a part of SMX disappeared in an unknown pathway when
190 denitrification started (25±5% and 45±2% in the BAR and NDL experiments, respectively)
191 whereas the remainder was fully transformed into 4-nitro-SMX and desamino-SMX. These two
192 compounds were unstable metabolites that were re-transformed into SMX, the parent
193 compound, when nitrate and nitrite were (almost completely) depleted.

194 **2.1.2.2 Conceptualization**

195 The generation of the two metabolites 4-nitro-SMX and desamino-SMX in the BAR experiment
196 was ascribed to the denitrification activity enhanced by the presence of a large external source
197 of organic carbon. In both metabolites the key point is the substitution of the primary amine of
198 sulfamethoxazole by different radicals. The formation of 4-nitro-SMX implies the nitrosation of
199 the primary amine of SMX, whereas desamino-SMX involves the deamination process again of
200 the primary amine. From these considerations, we propose the next conceptual model
201 (summarized in Figure S1 of Supplementary Material).

202 The occurrence of either nitrosation or deamination of the primary amine could be
203 attributed to the presence of nitrous acid, the conjugate (weak) acid of nitrite (with pKa = 3.15
204 at 25ºC, see Morrisson and Boyd (1992)). The presence of nitrous acid facilitated the formation

of a diazonium cation replacing the amine radical in SMX. This compound was not stable under ambient conditions and thus, could undergo numerous and consecutive fast reactions, strongly depending on reaction conditions and available reaction partners (Carey and Sundberg 2007, Morrisson and Boyd 1992). One reaction path consisted of the diazonium molecule reacting again with another acid nitrous molecule forming 4-nitro-SMX. A second path implied the reaction of the diazonium molecule with an alcohol (methanol was present in the batch experiment), forming a desamino-SMX molecule (Everett 1973). All the reactions paths and the molecules proposed are sketched in Figure S1 of Supplementary Material.

Note that the formation of 4-nitro-SMX and desamino-SMX were both driven by the presence of HNO_2, a subproduct of the denitrification process. Nevertheless, the reaction of degradation of SMX was abiotic, meaning that SMX did not participate in the denitrifying metabolism. Thus, the co-metabolic pathway of degradation consisted in the generation of nitrite as an intermediate product of the denitrifying metabolism. At that point, nitrite was conjugated with H^+ and formed HNO_2 which was the responsible to generate an abiotic reaction with a diazonium salt as an intermediate product, and the last responsible of the observed decay (and virtual disappearance) of SMX concentrations.

The retransformation of 4-nitro-SMX into SMX was confirmed by a supplementary experiment in Nödler et al. (2012), which proved the reduction of 4-nitro-SMX to its corresponding amino-compound (SMX) in the absence of denitrification. The molecular mechanism proposed is reductive degradation, similar to the degradation of nitrobenze to aniline (Figure S2 Supplementary Material), involving an overall inclusion of $6H^+$ and the removal of $2H_2O$ molecules. The reductive degradation could be mediated biotically (e.g., Peres et al. 1998) or abiotically, with no information available to allow discriminating between them.

Concerning the fate of desamino-SMX and considering the mass balance in the NDL experiment, it seemed logical to infer that it was also retransformed into SMX. The most

common mechanism for the reintroduction of nitrogen functionality into aromatic rings (in form of nitro radical) is nitration, which would imply creating a nitro-aromatic compound, here again 4-nitro-SMX. After that, the nitro compound could be reduced easily to the corresponding amino derivatives, as conceptualized by Carey and Sundberg 2007 and Nödler et al. 2012. The active nitrating species would be the nitronium ion, NO_2^+ (Carey and Sundberg 2007), which would be formed by the protonation and dissociation of nitric acid in the presence of sulfuric acid, acting as a catalyzer (Figure S3, Supplementary Material). As these two compounds were present in the BAR and NDL experiments at similar concentrations of SMX, this is a plausible mechanism.

To sum up, the complete conceptual model of SMX under denitrifying conditions would imply the formation of two metabolites (4-nitro-SMX and desamino-SMX), which are not stable and are retransformed to the parent compound, directly in the case of 4-nitro-SMX or with a previous transformation to nitro compound for desamino-SMX. The full reaction chain is summarized in Figure 3.

2.1.3 SMX behavior under Fe reducing conditions. Observations and process inference

Degradation of SMX under iron reducing conditions was described in Mohatt et al. (2011) based on experimental work. The authors proposed a process based on the electron flow produced by the re-oxidation of ferrous iron (II) to ferric iron (III) taking place on the surface of goethite, which facilitates the break of the SMX molecule. As Fe(II) was previously produced by biological reduction of Fe(III), the degradation of SMX occurred, again, as a result of a co-metabolism process initiated by labile organic carbon degradation.

The conceptualization of this degradation process is summarized in Figure 4. The metabolite formed is the result of the breakage of the isoxazole ring. Following this break, four metabolites can be formed (see Table 3), each one following a particular degradation pathway (Mohatt et al. 2011).

Note that depending on the existing redox state, the metabolites generated are very different. Whereas during denitrification the metabolites formed involve the reversible substitution of the amine radical, during either aerobic or iron reduction conditions the isoxazole ring is irreversibly broken, thus facilitating the eventual mineralization of SMX.

2.2 Model development

2.2.1 Modeling co-metabolic degradation of SMX: coupling denitrification model with SMX degradation and metabolite formation

As indicated in the conceptual model, we postulate that the key abiotic process controlling the degradation of the SMX in the experiments was the presence of nitrous acid linked to nitrite accumulation. The first modelling step consisted in the development of a biodenitrification model capable of accounting for the transient accumulation of nitrite, and subsequently the presence of nitrous acid. The model considered a multiple-Monod expression incorporating two terms: one for the electron donor (organic carbon) and another one for the electron acceptor, as well as two reduction steps: (1) nitrate to nitrite, and (2) nitrite to dinitrogen gas (see the matrix of rates and components in Table 4 and the complete denitrification reactions in Supplementary Material). The general Monod expression for electron donor was:

$$r = K_{\max} \frac{[ED]}{[ED] + k_{s,ED}} \frac{[EA]}{[EA] + k_{s,EA}} \frac{k_I}{[I] + k_I} [X] \quad (1)$$

where [*ED*] was the concentration of the electron donor (organic carbon), [$M_{ED}\ L^{-3}$]. [*EA*] that of the electron acceptor (nitrate or nitrite, *[*$M_{EA}\ L^{-3}$*]*), and [X] the biomass concentration *[*$M_X\ L^{-3}$*]*. K_{max} [$M_{Corg}\ M_{Corg,X}^{-1}\ T^{-1}$] was the maximum consumption rate of electron donor; and $K_{s\ EA}$ and $K_{s\ ED}$ [ML^{-3}] were half-saturation constants. The rate for the other components (electron acceptor and biomass) was expression (1) times the stoichiometric coefficients, Y_h (microbial yield, for biomass and electron donor) and *Q* (for electron acceptor and electron donor). As the presence of nitrate limits the reduction of nitrite (Almeida et al. 1995), an inhibition factor

accounting for the presence of NO_3, $[I]$ in [$M_I\ L^{-3}$], was added to the electron donor rate, with a constant k_I [ML^{-3}].

The time evolution of denitrifying biomass was not measured. For simplicity, it was considered constant in time, but active only after a certain elapsed time (lag phase). The actual value was 1 mM, consistent with available models of denitrification in batch experiments (Rodríguez-Escales et al. 2014). The lag phases were 1.8 and 3 days corresponding to the period of inactive biomass for the BAR and NDL experiments, respectively. Nitrous acid concentration was calculated considering its equilibrium with nitrite and a pKa of 3.15 (expression 3 at Table 4). On the other hand, nitric acid concentration was assumed equal to the proton concentration since this acid is strong and its concentration depends on the limiting former (protons in this case).

The rate expressions of SMX metabolite formation were defined for each one of the processes already conceptualized in Section 2.2 and Table 4. The formation of 4-nitro-SMX was modelled as second-order with respect to nitrous acid (proportional to the square of the concentration) and as a first-order (linear) with respect to the SMX concentration, resulting in a global third-order expression. On the other hand, desamino-SMX formation was modelled as a third-order kinetic expression, being first-order with respect to organic matter (methanol), nitrous acid and SMX (see Table 4 for the actual expressions). The retransformation of 4-nitro-SMX into SMX was modelled as a first-order degradation with respect to the metabolite. This model was previously applied in a side experiment of Nödler et al. (2012), where 4-nitro-SMX was converted into SMX in absence of denitrifying conditions and oxygen. Finally, the retransformation of desamino-SMX into the nitro compound was considered first-order with respect to the nitric acid and the metabolite, resulting in a second-order expression. The election of these rates orders was the outcome of the calibration process including the development of an appropriate conceptual model. Note that the order of the described expressions matched to the stoichiometry of the reactions for abiotic and not catalyzed

reactions (see Figure S1 from Supplementary Material and Table 4). Denoting the concentrations of sulfamethoxazole, 4-nitro-SMX and desamino-SMX respectively as $[SMX]$, $[4-NIT]$, and $[DES]$, the corresponding driving equations read

$$\frac{d[4-NIT]}{dt} = k_1[SMX][HNO_2]^2 - k_3[4-NIT] + k_4[DES][HNO_3] \quad (9)$$

$$\frac{d[DES]}{dt} = k_2[SMX][HNO_2][C_{org}]P - k_4[DES][HNO_3]. \quad (10)$$

In (2) and (3) all concentrations were expressed in [ML^{-3}]. Additional concentrations in these equations are $[HNO_2]$, $[HNO_3]$, $[C_{org}]$, respectively standing for nitrous acid, nitric acid, and labile organic carbon. The different parameters involved are k_1, k_2 [both in $L^6\ M^{-2}\ T^{1}$], k_3 [T^{-1}], and k_4 [$L^3\ M^{-1}\ T^{1}$]; P is the portion of methanol in the organic matter, 0.43 in BAR and 0.94 in NDL. Note that the rate of SMX would be equal to the sum of (9) and (10) with a change of sign, as we assume $[SMX] + [4-NIT] + [DES] = [SMX]_0$ (that is, the initial concentration of SMX).

Regarding the parameters of the model, the stoichiometric ones were determined from the reactions of denitrification (Table 4 and Section 2 of Supplementary Material). The kinetic parameters ($K_{\max}, k_s, k_i$ for the denitrification model, and k_1, k_2, k_3, k_4 for the SMX degradation model) were automatically calibrated using code PEST (Doherty 2005). Notice that this process involved two independent (not simultaneous) calibration processes. PEST code allowed computing the sensitivities, correlations, and linear uncertainties (confidence intervals) for the optimized model parameters using the Levenberg-Marquardt algorithm. The weights of each chemical species (ω_i) associated to the measurement errors (ε_i) were applied using the inverse of the standard deviation of the confidence interval of measurements (95%). For the calibration process, we used the experimental information (nitrate, nitrite, SMX, 4-nitro-SMX and desamino-SMX) provided by Barbieri et al. (2012) and Nödler et al. (2012). The initial concentrations of the model are summarized in Table 2. Note that the initial concentration of

330 SMX in the model of NDL experiment represented 45% of the initial one (1.8 µM). This was
331 because the concentration of SMX suddenly decreased during the lag phase (Figure 2).
332 Afterwards the mass balance remained constant.

333 **2.2.2 Mathematical model and application to the interpretation of experiments of SMX**
334 **under iron reducing conditions**

335 The original model of SMX degradation under iron reducing conditions proposed by Mohatt et
336 al. (2011) assumes an exponential decay for SMX, focusing on a single abiotic degradation
337 process. Our conceptual model is based on the reaction occurring on the surface of goethite,
338 having a significantly different behavior at early times and at late times. At early times the
339 exponential model fits properly the experimental data of Mohatt et al. (2011); this implies that
340 the model is based on a large number of available sites for reaction at the goethite surface.
341 Once these sites are mostly exhausted (intermediate to large times), additional ones must be
342 found at deeper layers. The number of sites at those deep layers can be best modeled using a
343 fractal approach, so that the reaction rate is best described by a power law. Thus, the
344 governing equations are:

345 $$\frac{d[SMX]}{dt} = \begin{cases} -k_5[SMX] \\ -k_6[SMX]^n \end{cases} \quad (11)$$

346 where k_5 [T^{-1}] and k_6 [$M^{1-n}L^{3n-3}T^{-1}$] are degradation constants. The top expression in (11) is
347 applicable for short times and the bottom one would be valid for intermediate to large times,
348 with a transition of behavior not clearly defined.

349

350 **3 Results and discussion**

351 **3.1 Fate of SMX and metabolites under denitrifying and iron reducing conditions**

352 Figure 2 displays the results of the modelling effort applied to the BAR (top row) and NDL
353 (bottom) using the best-fitted parameters listed in Table 5. Figures 2a and 2d correspond to

354 the biodenitrification process in terms of nitrate and nitrite concentrations. The corresponding
355 inferred (not measured) presence of nitrous acid is displayed in Figures 2b and 2e. These same
356 plots present the model fit of the concentrations of SMX and the two metabolites (only one in
357 the BAR experiment). SMX concentrations are reasonably well reproduced with the only
358 exception of the last point in the BAR experiment; we associate this misfit to the model not
359 accounting for iron/manganese reduction conditions developing after 10 days. Regarding the
360 concentration of 4-nitro-SMX, the model reproduced quantitatively the temporal behavior in
361 both experiments. In addition desamino-SMX concentrations were well reproduced for the
362 NDL experiment (in the BAR experiment, Figure 2b, this value was only inferred, and plotted as
363 a green dashed line).

364 The results of the calibration of the SMX degradation model are displayed in Table 5. The
365 parameters inferred display a high degree of uncertainty, being larger in the BAR experiment.
366 This is probably due to the lack of measurements regarding one of the metabolites (desamino-
367 SMX), affecting the values of k_2, k_4 through equation (2), with such uncertainty propagating
368 to k_1 and k_3. Furthermore, the correlation matrix displayed by PEST showed that there was
369 no correlation among the parameters (all values were lower than 0.55, results not shown).

370 Note that despite modeling the same processes in the two experiments, the parameters
371 determined in BAR and NDL are quite different being higher in the former (for example k_1 and
372 k_2 are two orders of magnitude higher). All but first-order degradation rates (third-order in the
373 nitrosation of the primary amines and second-order in the nitration of the benzene ring) are
374 dependent on initial conditions (Atkins and de Paula 2011). As the initial conditions were three
375 orders of magnitude different, it is evident that the parameters were not able to be compared.
376 Furthermore, the high concentration of SMX in NDL experiment could represent some type of
377 biomass inhibition and could be another reason for such differences. Nevertheless, we did not
378 have enough experimental data to characterize if this existed and if it had any consequence.

379 Regarding the degradation of SMX under iron-reducing conditions, the best fit was
380 obtained using the automatically calibrated by PEST parameters (see section 3.1.1) and they
381 are listed in Table 5, and the actual fit to data is displayed in Figure 5. Actually, in the same
382 Figure the fit with an exponential model is also presented, here focused only on early time
383 data, to show the transition in behavior as a function of time. Note that all potential
384 degradation pathways described would be naturally limited by the low amount of organic
385 carbon in the subsoil. Besides this, iron-reducing conditions will only be reached when all the
386 previous redox states were ended. Thus, the amount of organic carbon supplied to the system
387 is key. Once iron reducing conditions were achieved, the degradation of SMX is achieved in
388 hours (Figure 5).

389 **3.2 Potential extensions to real field site applications**

390 The main reactive path for the degradation of SMX under denitrifying conditions involves the
391 presence of nitrous acid that accumulates associated with the building up (and further decay)
392 of nitrite. Nitrite is a usual transient compound in denitrification processes. Its accumulation
393 can be, traditionally, explained by different reasons: 1) the presence of low levels of oxygen
394 (up to 0.7 mg/l) (Coyne and Tiedje 1990); 2) the competition between nitrate and nitrite
395 enzymes for a common electron donor (Thomsen et al. 1990); 3) large differences in the
396 maximum reduction rates of nitrate and nitrite reductases (Betlach and Tiedje 1981); and 4)
397 the choice of carbon source (van Rijn et al. 1996). In addition, the presence of antibiotics is
398 suggested to inhibit the reduction step from nitrate to nitrite (Yan et al. 2013), and thus
399 facilitate nitrite accumulation and nitrous acid formation. Other studies also suggested that a
400 continuous exposition to SMX in large quantities will affect the bacterial denitrifying
401 community (Underwood et al. 2011). Consequently, the presence of 4-nitro-SMX would be
402 quite plausible in natural aqueous environments where nitrate and antibiotics leakage
403 converge, such as rural areas where nitrate and veterinarian antibiotics coexist (García-Galán
404 et al. 2010). As the formation of desamino-SMX will be conditioned to the presence of alcohol

405 which is not always present in organic matter, we expect that in real site applications 4-nitro-
406 SMX will be the dominant metabolite. If we consider that alcohol and, therefore, desamino-
407 SMX are not present, we could assume that SMX would only transition to 4-nitro-SMX.

408 There is an increasing concern in the possibility that metabolites produced during the
409 degradation of emerging compounds will be more hazardous to either human health or
410 ecosystem than the parent itself. For that, we compared the LC_{50} for *Daphnia sp.* (after 48 h)
411 and fish (after 96 h) calculated by ECOSAR packet of EPI-SUITE (USEPA 2012), for all
412 metabolites evaluated in this work (Table 6). Both *Daphnia sp.* and fish were used as proxys of
413 the full ecosystem. In Table 6 we have also included partition coefficients as well as solubility
414 for each compound in order to compare the impact to the environment. Although the
415 presented concentrations of toxicity are referred to the acute toxicity and they are much
416 higher than the environmental concentrations of SMX, they serve as a comparative criterion.
417 Overall, 4-nitro-SMX was the most toxic compound (lowest LC_{50}). The toxicity was associated
418 to the nitroaromatic compounds which are acutely toxic and mutagenic, and many are
419 suspected or established carcinogens (Ju and Parales 2010). On the other hand, metabolites
420 conserving the isoxazole ring (Product II in Table 3 and 3-amino-5-methylisoxazole) are more
421 toxic when compared to SMX. Contrarily, 4-aminobenzosulfonate and metabolites produced
422 under iron reducing conditions with broken isoxazole ring (Products III and IV in Table 3) are
423 the least toxic of all the compounds studied, and probably they can be mineralized easily (Gao
424 et al. 2010). These results are perfectly correlated with values of $\log K_{ow}$ and solubility. The
425 highest values of $\log K_{ow}$ correlated to the highest value of LC_{50}, and at the same time, the
426 highest values of solubility correspond to low risk compounds. High solubility and low values of
427 K_{ow} indicate that all the metabolites will remain mainly in water, with low absorptivity rates
428 into solid phases.

429 From the combination of reversibility and environmental fate/risk, it seems reasonable
430 to conclude that the most efficient degradation path to remove all presence of SMX from

groundwater bodies involves allowing the aquifer to reach iron reducing conditions. We want to stress here that this conclusion is only valid for SMX, and thus a potential intelligent methodology to eliminate a cocktail of emerging organic compound and their metabolites would be to allow the aquifer to reach many different redox states, each one of them being the most efficient one for the degradation of a given molecule. At this point there is a need in the future to investigate many more molecules and even the synergic effect of injecting several compounds together.

In any case, and indistinctly to the redox process, the degradation of SMX is driven by co-metabolism enhanced by the presence of external labile organic carbon. In this way, it might be possible to properly manage the amount of labile organic carbon in the system, thus properly allowing the control (in space and time) of redox zonation for the proper management of EOCs degradation in the subsurface. One real example of this application is the installation of a labile organic carbon layer (compost) on the bottom of an infiltration pond in a managed aquifer recharge facility that enhanced EOCs degradation (Schaffer et al. 2015, Valhondo et al. 2014, Valhondo et al. 2015). The induced redox zonation by the oxidation of labile organic carbon increased the possibilities of degradation of different emerging compounds, here including sulfamethoxazole.

4 Conclusions

In this work we have conceptualized and modelled the degradation path of the SMX (sulfamethoxazole) molecule under different redox conditions in groundwater. We have developed a model capable of reproducing the fate of SMX as well as its metabolites under different redox conditions. Our model is based on the understanding of the real molecular mechanism of degradation instead of using simplified models postulating first-order degradation models, based on the apparent degradation behavior of SMX in experiments.

Our model focused on denitrifying and iron-reducing conditions, being the dominant ones for SMX degradation in groundwater. The main reactive path for the degradation of SMX under denitrification involves the presence of nitrous acid, which promotes the nitrosation of the primary amine of SMX forming 4-nitro-SMX. If alcohol is present in the system a second metabolite is produced, desamino-SMX. Both of them are unstable and can eventually be retransformed to the parent compound. Biologically iron reduction conditions would facilitate the break of the SMX molecule through enhancing the abiotic mechanism of oxidation of ferrous iron to ferric iron. Several metabolites may be formed, involving the break of the isoxazole ring in the SMX molecule and individual potential degradation pathways.

The mathematical model proposed for SMX degradation under denitrifying conditions involves different forward and backward processes with complex kinetic rates. For 4-nitro-SMX two forward processes arise, one involving SMX and the concentration of HNO_2 squared, and a second one proportional to the concentration of desamino-SMX and also to that of HNO_3. The backward term implies linear first-order degradation. For desamino-SMX there is one forward term, proportional to the concentrations of SMX, HNO_2 and organic carbon in the form of alcohol, and a backward one proportional to the concentrations of desamino-SMX and HNO_3.

The model presented is capable of properly reproducing the results from two experiments reported in the literature. The actual parameters present in the governing equations are strongly influenced by the initial concentration of the SMX. In the case of iron reducing conditions it was found that the best reproduction of a batch experiment is obtained by a combination of an exponential model at short times and a power law function at large times.

The shortest reported characteristic time for degradation of the SMX molecule corresponds to iron reducing conditions. Also, in this case, it was found that the metabolites produced under iron reducing conditions are the most convenient in terms of minimizing total risk to ecosystems. The work performed in SMX could be extended to other EOCs, and each

482 one of them is expected to behave differently and to be best degraded for some specific redox
483 conditions. Thus, in real field applications the optimal combination to degrade a suite of EOCs
484 would be to enhance redox zonation by an engineered introduction of organic carbon in the
485 aquifer.

486 5 Acknowledgements

487 We thank the three reviewers and the associate editor for their comments and suggestions,
488 which helped improve the quality of the manuscript. Financial support was provided by the
489 European Union, project MARSOL FP7-ENV-2013-WATER-INNO-DEMO and by Spanish
490 government, project INDEMNE, CGL2015-69768-R. XSV acknowledges support by the ICREA
491 Academia Program.

492 6 References

493 Almeida, J.S., Reis, M.A. and Carrondo, M.J. (1995) Competition between nitrate and nitrite
494 reduction in denitrification by *Pseudomonas fluorescens.* Biotechnol. Bioeng. 46(5), 476-
495 484.
496 Atkins, P. and de Paula, J. (2011) Physical Chemistry for the life sciences. Second edition.
497 Banzhaf, S., Nödler, K., Licha, T., Krein, A. and Scheytt, T. (2012) Redox-sensitivity and mobility
498 of selected pharmaceutical compounds in a low flow column experiment. Sci. Total Environ.
499 438(0), 113-121.
500 Barbieri, M., Carrera, J., Ayora, C., Sanchez-Vila, X., Licha, T., Nodler, K., Osorio, V., Perez, S.,
501 Kock-Schulmeyer, M., Lopez de Alda, M. and Barcelo, D. (2012) Formation of diclofenac and
502 sulfamethoxazole reversible transformation products in aquifer material under denitrifying
503 conditions: batch experiments. Sci. Total Environ. 426, 256-263.
504 Barbieri, M., Carrera, J., Sanchez-Vila, X., Ayora, C., Cama, J., Köck-Schulmeyer, M., López de
505 Alda, M., Barceló, D., Tobella Brunet, J. and Hernández García, M. (2011) Microcosm

experiments to control anaerobic redox conditions when studying the fate of organic micropollutants in aquifer material. J. Contam. Hydrol. 126(3–4), 330-345.

Baumgarten, B., Jährig, J., Reemtsma, T. and Jekel, M. (2011) Long term laboratory column experiments to simulate bank filtration: Factors controlling removal of sulfamethoxazole. Water Res. 45(1), 211-220.

Betlach, M.R. and Tiedje, J.M. (1981) Kinetic explanation for accumulation of nitrite, nitric oxide, and nitrous oxide during bacterial denitrification. Applied and Environmental Microbiology 42(6), 10.

Carey, F.A. and Sundberg, R.J. (2007) Advanced Organic Chemistry. Part B: Reactions and Synthesis., Springer.

Coyne, M.S. and Tiedje, J.M. (1990) Induction of denitrifying enzymes in oxygen-limited Achromobacter cycloclastes continuous culture. FEMS Microbiology Letters 73(3), 263-270.

Doherty, J. (2005) PEST: model independent parameter estimation. Watermark Numerical Computing, fifth edition of user manual.

Drillia, P., Dokianakis, S.N., Fountoulakis, M.S., Kornaros, M., Stamatelatou, K. and Lyberatos, G. (2005) On the occasional biodegradation of pharmaceuticals in the activated sludge process: The example of the antibiotic sulfamethoxazole. Journal of Hazardous Materials 122(3), 259-265.

Everett, M. (1973) Deamination by the diazotization-deazotization method. Histochem. J. 5(1), 1-7.

Fent, K., Weston, A.A. and Caminada, D. (2006) Ecotoxicology of human pharmaceuticals. Aquat. Toxicol. 76(2), 122-159.

Gao, J., Ellis, L.B.M. and Wackett, L.P. (2010) The University of Minnesota Biocatalysis/Biodegradation Database: improving public access. Nucleic Acid Res 38(suppl 1), D488-D491.

531 Gao, S., Zhao, Z., Xu, Y., Tian, J., Qi, H., Lin, W. and Cui, F. (2014) Oxidation of sulfamethoxazole
532 (SMX) by chlorine, ozone and permanganate—A comparative study. J. Hazard. Mat. 274(0),
533 258-269.
534 García-Galán, M.J., Garrido, T., Fraile, J., Ginebreda, A., Díaz-Cruz, M.S. and Barceló, D. (2010)
535 Simultaneous occurrence of nitrates and sulfonamide antibiotics in two ground water
536 bodies of Catalonia (Spain). J. Hydrol. 383(1–2), 93-101.
537 Gauthier, H., Yargeau, V. and Cooper, D.G. (2010) Biodegradation of pharmaceuticals by
538 Rhodococcus rhodochrous and Aspergillus niger by co-metabolism. Science of The Total
539 Environment 408(7), 1701-1706.
540 Gavrilescu, M., Demnerová, K., Aamand, J., Agathos, S. and Fava, F. (2015) Emerging pollutants
541 in the environment: present and future challenges in biomonitoring, ecological risks and
542 bioremediation. New Biotechnol. 32(1), 147-156.
543 Greskowiak, J., Prommer, H., Massmann, G. and Nützmann, G. (2006) Modeling Seasonal
544 Redox Dynamics and the Corresponding Fate of the Pharmaceutical Residue Phenazone
545 During Artificial Recharge of Groundwater. Environ. Sci. Technol. 40(21), 6615-6621.
546 Grünheid, S., Amy, G. and Jekel, M. (2005) Removal of bulk dissolved organic carbon (DOC) and
547 trace organic compounds by bank filtration and artificial recharge. Water Res. 39(14), 3219-
548 3228.
549 Göbel, A., Thomsen, A., McArdell, C.S., Joss, A. and Giger, W. (2005) Occurrence and Sorption
550 Behavior of Sulfonamides, Macrolides, and Trimethoprim in Activated Sludge Treatment.
551 Environ. Sci. Technol. 39(11), 3981-3989.
552 Heberer, T. (2002) Occurrence, fate, and removal of pharmaceutical residues in the aquatic
553 environment: a review of recent research data. Toxicol. Lett. 131(1–2), 5-17.
554 Heberer, T., Massmann, G., Fanck, B., Taute, T. and Dünnbier, U. (2008) Behaviour and redox
555 sensitivity of antimicrobial residues during bank filtration. Chemosphere 73(4), 451-460.

556 Henzler, A.F., Greskowiak, J. and Massmann, G. (2014) Modeling the fate of organic
557 micropollutants during river bank filtration (Berlin, Germany). J. Contam. Hydrol. 156(0), 78-
558 92.
559 Hirsch, R., Ternes, T., Haberer, K. and Kratz, K.-L. (1999) Occurrence of antibiotics in the aquatic
560 environment. Sci. Total Environ. 225(1–2), 109-118.
561 Ji, Y., Ferronato, C., Salvador, A., Yang, X. and Chovelon, J.M. (2014) Degradation of
562 ciprofloxacin and sulfamethoxazole by ferrous-activated persulfate: implications for
563 remediation of groundwater contaminated by antibiotics. Sci. Total Environ. 472, 800-808.
564 Jjemba, P.K. (2002) The potential impact of veterinary and human therapeutic agents in
565 manure and biosolids on plants grown on arable land: a review. Agr. Ecosyst. Enviro. 93(1–
566 3), 267-278.
567 Ju, K.-S. and Parales, R.E. (2010) Nitroaromatic Compounds, from Synthesis to Biodegradation.
568 Microbiol Mol Biol Rev. 74(2), 250-272.
569 Liu, Y.-S., Ying, G.-G., Shareef, A. and Kookana, R.S. (2013) Biodegradation of three selected
570 benzotriazoles in aquifer materials under aerobic and anaerobic conditions. J. Contam.
571 Hydrol. 151, 131-139.
572 Mohatt, J.L., Hu, L., Finneran, K.T. and Strathmann, T.J. (2011) Microbially mediated abiotic
573 transformation of the antimicrobial agent sulfamethoxazole under iron-reducing soil
574 conditions. Environ. Sci. Technol. 45(11), 4793-4801.
575 Morrisson, R.T. and Boyd, R.N. (1992) Organic Chemistry, 6th edition, Prentice-Hall, Inc. A
576 Paramount Communications Company.
577 Müller, E., Schüssler, W., Horn, H. and Lemmer, H. (2013) Aerobic biodegradation of the
578 sulfonamide antibiotic sulfamethoxazole by activated sludge applied as co-substrate and
579 sole carbon and nitrogen source. Chemosphere 92(8), 969-978.

580 Nham, H.T.T., Greskowiak, J., Nödler, K., Rahman, M.A., Spachos, T., Rusteberg, B., Massmann,
581 G., Sauter, M. and Licha, T. (2015) Modeling the transport behavior of 16 emerging organic
582 contaminants during soil aquifer treatment. Sci. Total Environ. 514(0), 450-458.
583 Nödler, K., Licha, T., Barbieri, M. and Pérez, S. (2012) Evidence for the microbially mediated
584 abiotic formation of reversible and non-reversible sulfamethoxazole transformation
585 products during denitrification. Water Res. 46(7), 2131-2139.
586 Peres, C.M., Naveau, H. and Agathos, S.N. (1998) Biodegradation of nitrobenzene by its
587 simultaneous reduction into aniline and mineralization of the aniline formed. Appl.
588 Microbiol. Biotechnol. 49(3), 343-349.
589 Reis, P.J.M., Reis, A.C., Ricken, B., Kolvenbach, B.A., Manaia, C.M., Corvini, P.F.X. and Nunes,
590 O.C. (2014) Biodegradation of sulfamethoxazole and other sulfonamides by Achromobacter
591 denitrificans PR1. J. Hazard. Mat. 280(0), 741-749.
592 Rodríguez-Escales, P., van Breukelen, B., Vidal-Gavilan, G., Soler, A. and Folch, A. (2014)
593 Integrated modeling of biogeochemical reactions and associated isotope fractionations at
594 batch scale: A tool to monitor enhanced biodenitrification applications. Chem. Geol. 365(0),
595 20-29.
596 Schaffer, M., Kröger, K.F., Nödler, K., Ayora, C., Carrera, J., Hernández, M. and Licha, T. (2015)
597 Influence of a compost layer on the attenuation of 28 selected organic micropollutants
598 under realistic soil aquifer treatment conditions: Insights from a large scale column
599 experiment. Water Res. 74(0), 110-121.
600 Schwarzenbach, R.P., Escher, B.I., Fenner, K., Hofstetter, T.B., Johnson, C.A., von Gunten, U.
601 and Wehrli, B. (2006) The Challenge of Micropollutants in Aquatic Systems. Science
602 313(5790), 1072-1077.
603 Stadler, L.B., Su, L., Moline, C.J., Ernstoff, A.S., Aga, D.S. and Love, N.G. (2015) Effect of redox
604 conditions on pharmaceutical loss during biological wastewater treatment using sequencing
605 batch reactors. J. Hazard. Mater. 282, 106-115.

606 Szczepanowski, R., Linke, B., Krahn, I., Gartemann, K.H., Gutzkow, T., Eichler, W., Puhler, A. and
607 Schluter, A. (2009) Detection of 140 clinically relevant antibiotic-resistance genes in the
608 plasmid metagenome of wastewater treatment plant bacteria showing reduced
609 susceptibility to selected antibiotics. Microbiology 155(Pt 7), 2306-2319.
610 Thomsen, J.K., Geset, T. and Cox, R.P. (1990) Mass spectrometric studies of the effect of pH on
611 the accumulation of intermediates in denitrification byParacoccus denitrificans. Applied
612 Environmental Microbiology 60(2), 5.
613 Underwood, J.C., Harvey, R.W., Metge, D.W., Repert, D.A., Baumgartner, L.K., Smith, R.L.,
614 Roane, T.M. and Barber, L.B. (2011) Effects of the Antimicrobial Sulfamethoxazole on
615 Groundwater Bacterial Enrichment. Environ. Sci. Technol. 45(7), 3096-3101.
616 USEPA (2012) Estimation Programs Interface Suite™ for Microsoft® Windows.
617 Valhondo, C., Carrera, J., Ayora, C., Barbieri, M., Nodler, K., Licha, T. and Huerta, M. (2014)
618 Behavior of nine selected emerging trace organic contaminants in an artificial recharge
619 system supplemented with a reactive barrier. Environ. Sci. Pollut. Res. Int. 21(20), 11832-
620 11843.
621 Valhondo, C., Carrera, J., Ayora, C., Tubau, I., Martinez-Landa, L., Nödler, K. and Licha, T. (2015)
622 Characterizing redox conditions and monitoring attenuation of selected pharmaceuticals
623 during artificial recharge through a reactive layer. Sci. Tot. Environ. 512–513(0), 240-250.
624 van Rijn, J., Tal, Y. and Barak, Y. (1996) Influence of Volatile Fatty Acids on Nitrite Accumulation
625 by a Pseudomonas. Appl. Environ. Microbiol. 62(7), 2615-2620.
626 Yan, C., Dinh, Q.T., Chevreuil, M., Garnier, J., Roose-Amsaleg, C., Labadie, P. and Laverman,
627 A.M. (2013) The effect of environmental and therapeutic concentrations of antibiotics on
628 nitrate reduction rates in river sediment. Water Res. 47(11), 3654-3662.

629

630 **Figure captions**

631 **Figure 1.** Pathway of aerobic degradation of SMX proposed by Gao et al. (2010) and later
632 confirmed experimentally by Müller et al. (2013) and Reis et al. (2014).

633 **Figure 2.** Experimental information of Barbieri et al. (2012) (a, b, c) and Nödler et al. (2012) (d,
634 e, f) (points) and modelled results of nitrate and nitrite (a,d), sulfamethoxazole, 4-nitro
635 sulfamethoxazole, desamino-sulfamethoxazole and nitrous acid (b,d). The time axis is
636 displayed in log scale. The extremes of the bars associated with each individual measurement
637 indicate the values obtained from two replicates, while dots display their arithmetic average.
638 Solid lines represent the results from the modeling effort (Section 3.1). Dashed lines in b) and
639 e) represent expected (from the model) concentrations of non-measured elements.

640 **Figure 3.** Conceptual model of processes involved in the fate of SMX under denitrifying
641 conditions (italic letters) and the corresponding metabolites.

642 **Figure 4.** Conceptual model of SMX due to the abiotic oxidation of iron due to a previous
643 reduction of goethite biologically mediated (modified from Mohatt et al. (2011)).

644 **Figure5.** Experimental point (from Mohatt et al. (2011)) and modelling results using first-order
645 degradation rate and power law.

646

Table caption

Table 1. Compilation of values of degradation half-time reported in the literature for aerobic degradation of SMX assuming first-order reaction.

Table 2. Main compounds in the input water used in the BAR and NDL experiments. The complete hydrochemistry can be consulted in Barbieri et al. (2012) and Nödler et al. (2012).

Table 3. Metabolites of SMX detected during iron reducing conditions (modified from Mohatt et al. 2011).

Table 4. Processes, components and rates involved during degradation of SMX under denitrifying conditions. The stoichiometric coefficients were determined from complete reactions (Section 2 for denitrification and Fig. S1 and S2 for SMX under denitrifying conditions).

Table 5. Model parameters (mean and standard deviation, SD) used in denitrification model and SMX degradation models.

Table 6. Octanol partition coefficient, solubility and LC_{50} of SMX and all metabolites evaluated in this work. All these values were estimated using ECOSAR package of EPI-SUITE (USEPA 2012).

Table1

Click here to download Table: SMX_table1_v3.docx

Work	$T_{1/2}$ ($T_{1/2}$=ln2/k)	Experimental conditions
Baumgarten et al., 2011	1 - 9 d (calculated with biomass acclimated during 28 weeks of experiment)	Column experiment Aerobic surface water Concentrations of SMX were between 0.25 and 4.15 µg/L
Gauthier et al., 2010	35 d	Batch experiment (*R. rhodocrous*) Activated sludge with acclimated biomass Concentration of SMX was 31.6 mg/L
Reis et al., 2014	31, 34 and 99 d	Batch experiment Activated sludge with acclimated biomass Concentrations of SMX were between 152 and 2500 mg/L
Drillia et al., 2005	3.5 d (with acetate and nitrogen source), 10.5 d (without)	Batch experiment Concentration of SMX was 200 mg/L Activated sludge with acclimated biomass

Table2

Click here to download Table: SMX_table2_v3.docx

	Barbieri experiment (BAR)	Nödler experiment (NDL)
SMX (µM)	0.004	4
Nitrate (mM)	6.7	67.7
Organic carbon (mM)	9.7	71.5
Iron (Fe^{+3}) (mM)	0.001	0.001
Manganese (Mn^{+4}) (mM)	0.001	0.001
pH	8.5	7.3
Temperature (ºC)	25	25

Table3

Click here to download Table: SMX_table3_v3.docx

Product I 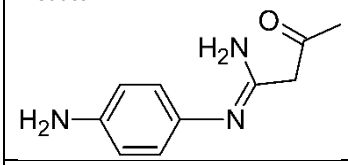	Product III 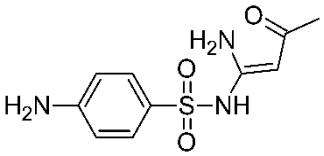
Product II 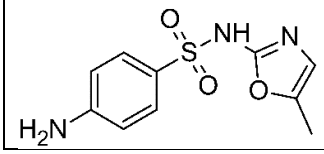	Product IV 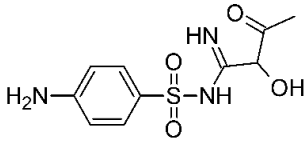

Table4

Click here to download Table: SMX_table4_v3.docx

Process	Components											Process rate	
	C_{org}	C_{inorg}	NO_3^-	NO_2^-	N_2	H^+	HNO_2	HNO_3	SMX	4-NIT	DESAM		
Organic matter degradation due to nitrate reduction	-1	+1	-2.2	+2.2								$K_{max}\frac{[C_{org}]}{[C_{org}]+k_{s,C_{org}}}\frac{[NO_3^-]}{[NO_3^-]+k_{s,NO_3^-}}[X]$	(2)
Organic matter degradation due to nitrite reduction	-1	+1		-1.5	+0.75	+1.5						$K_{max'}\frac{[C_{org}]}{[C_{org}]+k_{s',C_{org}}}\frac{[NO_2^-]}{[NO_2^-]+k_{s,NO_2^-}}\frac{k_I}{[NO_3^-]+k_I}[X]$	(3)
Nitrite equilibrium with nitrous acid				-1		-1	+1					$\frac{[NO_2^-][H^+]}{K_a}$	(4)
Nitrosation of primary amine and formation of 4-nitro-SMX							-2		-1	+1		$k_1[SMX][HNO_2]^2$	(5)
Nitrosation of primary amine and formation of desamino-SMX	-1						-1		-1		+1	$k_2[SMX][HNO_2][C_{org}]P$	(6)
Reduction of 4-nitro-SMX and formation of SMX									+1	-1		$k_3[4-NIT]$	(7)
Nitration of benzene ring of desamino-SMX and formation of 4-nitro-SMX								-1		+1	-1	$k_4[DES][HNO_3]$	(8)

Table5

Click here to download Table: SMX_table5_v3.docx

	Organic matter oxidation due to denitrification processes							
	Reduction of nitrate to nitrite		Reduction of nitrite to dinitrogen gas		Reduction of nitrate to nitrite		Reduction of nitrite to dinitrogen gas	
	Barbieri experiment				Nödler experiment			
	Mean	SD	Mean	SD	Mean	SD	Mean	SD
K_{max} ($molC_{org}/mol\ C_x\ d$)	19.0	3.6	11	1.1	2.0	0.8	2.0	0.5
k_{s,NO_3^-} (M)	1.0×10^{-4}	5.6×10^{-5}	-	-	3.0×10^{-3}	8.3×10^{-4}	-	-
k_{s,NO_2^-} $K_{s,NO2}$(M)	-	-	5.0×10^{-4}	4.8×10^{-4}	-	-	7.5×10^{-4}	5×10^{-4}
$k_{s,C_{org}}$ $K_{s\ Corg'}$ (M)	1.6×10^{-1}	3.9×10^{-2}	1.8×10^{-2}	1.0×10^{-2}	1.0×10^{-1}	1.1×10^{-2}	4.3×10^{-2}	1.4×10^{-2}
k_i (M)	-	-	5×10^{-4}	7×10^{-5}	-	-	3.5×10^{-1}	3.0×10^{-1}
	Abiotic degradation of SMX enhanced by co-metabolism (denitrification)							
	Barbieri experiment				Nödler experiment			
	Mean		SD		Mean		SD	
k_1 ($1/M^2$ d)	6.0×10^{14}		2.6×10^{15}		2.0×10^{12}		9.97×10^{11}	
k_2 ($1/M^2$ d)	1.3×10^{10}		6.8×10^{9}		8.8×10^{7}		7.5×10^{6}	
k_3 (1/d)	4.93		2.88		0.39		0.108	
k_4 (1/M d)	9.2×10^{6}		3.8×10^{5}		2.1×10^{6}		4.11×10^{5}	
	Abiotic degradation of SMX enhanced by co-metabolism (iron reducing conditions)							
k_5 (1/d)	2.7							
k_6 (1/d)	0.96							
n	0.91							

Table6

Click here to download Table: SMX_table6_v3.docx

	Conditions	$logK_{ow}$	Solubility (mg/L, 25ºC)	LC_{50} *Daphnia sp.*	LC_{50} fish
Sulfamethoxazole		0.89	$6.1x10^{2}$	$2.36x10^{2}$	$4.78x10^{3}$
4-amino benzosulfonate	Aerobic	-2.16	$5.7x10^{2}$	$2.57x10^{5}$	$6.59x10^{5}$
3-amino-5-methyl-isoxazole	Aerobic	0.22	$1.67x10^{5}$	$1.09x10^{3}$	$2.28x10^{3}$
4-nitro-sulfamethoxazole	Denitrifying	1.22	$5.67x10^{2}$	$6.18x10^{2}$	$1.17x10^{3}$
Desamino-sulfamethoxazole	Denitrifying	1.40	$1.75x10^{3}$	$3.63x10^{2}$	$6.75x10^{2}$
Product I	Iron reducing	0.19	3.35×10^{5}	$3.15x10^{3}$	$6.55x10^{3}$
Product II	Iron reducing	0.48	8.76×10^{3}	$2.36x10^{3}$	$4.78x10^{3}$
Product III	Iron reducing	-2.00	1×10^{6}	$3.21x10^{5}$	$8.18x10^{5}$
Product IV	Iron reducing	-4.17	1×10^{6}	$2.5x10^{7}$	$7.8x10^{7}$

Figure1

Click here to download high resolution image

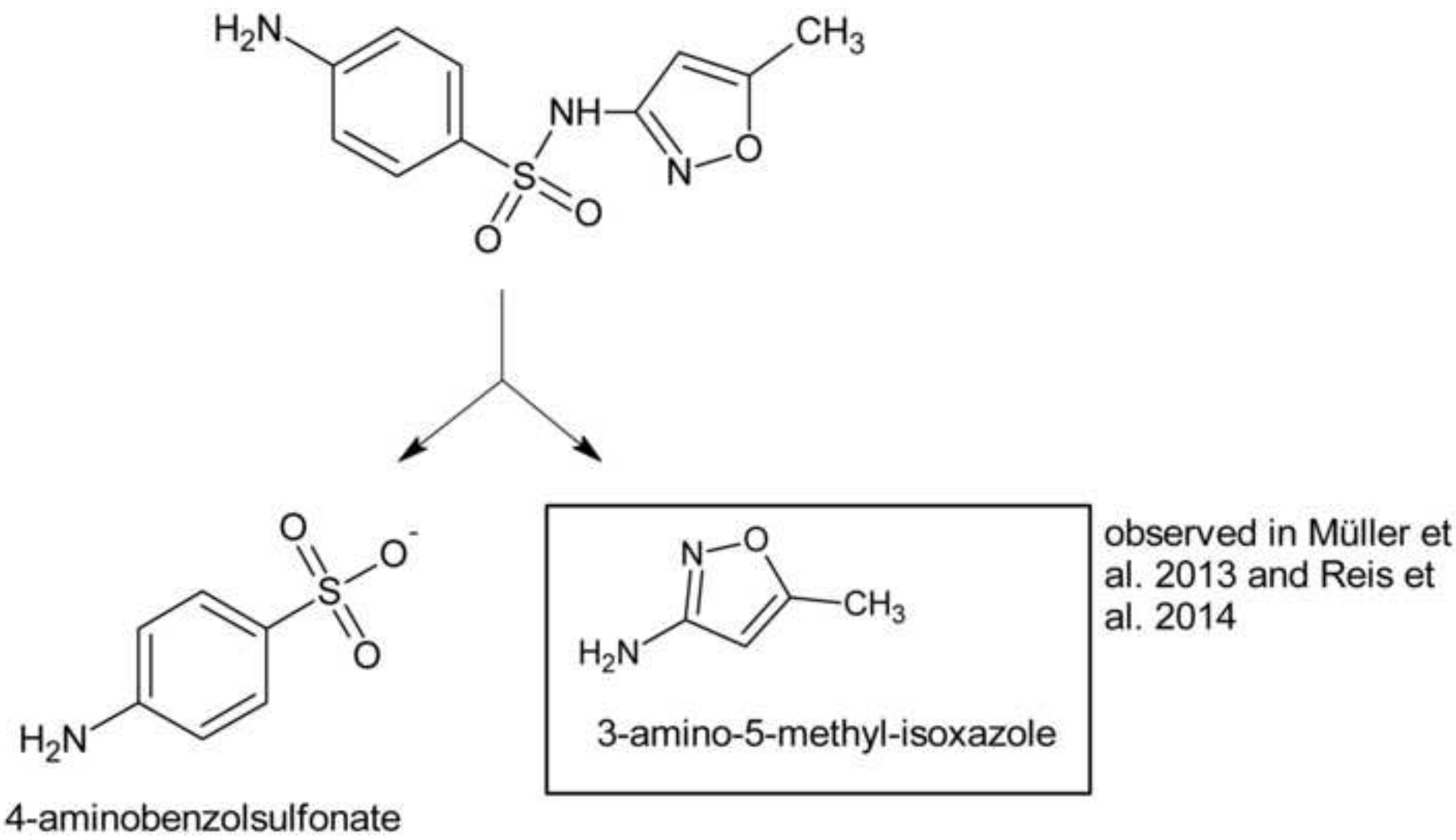

Figure2

Click here to download high resolution image

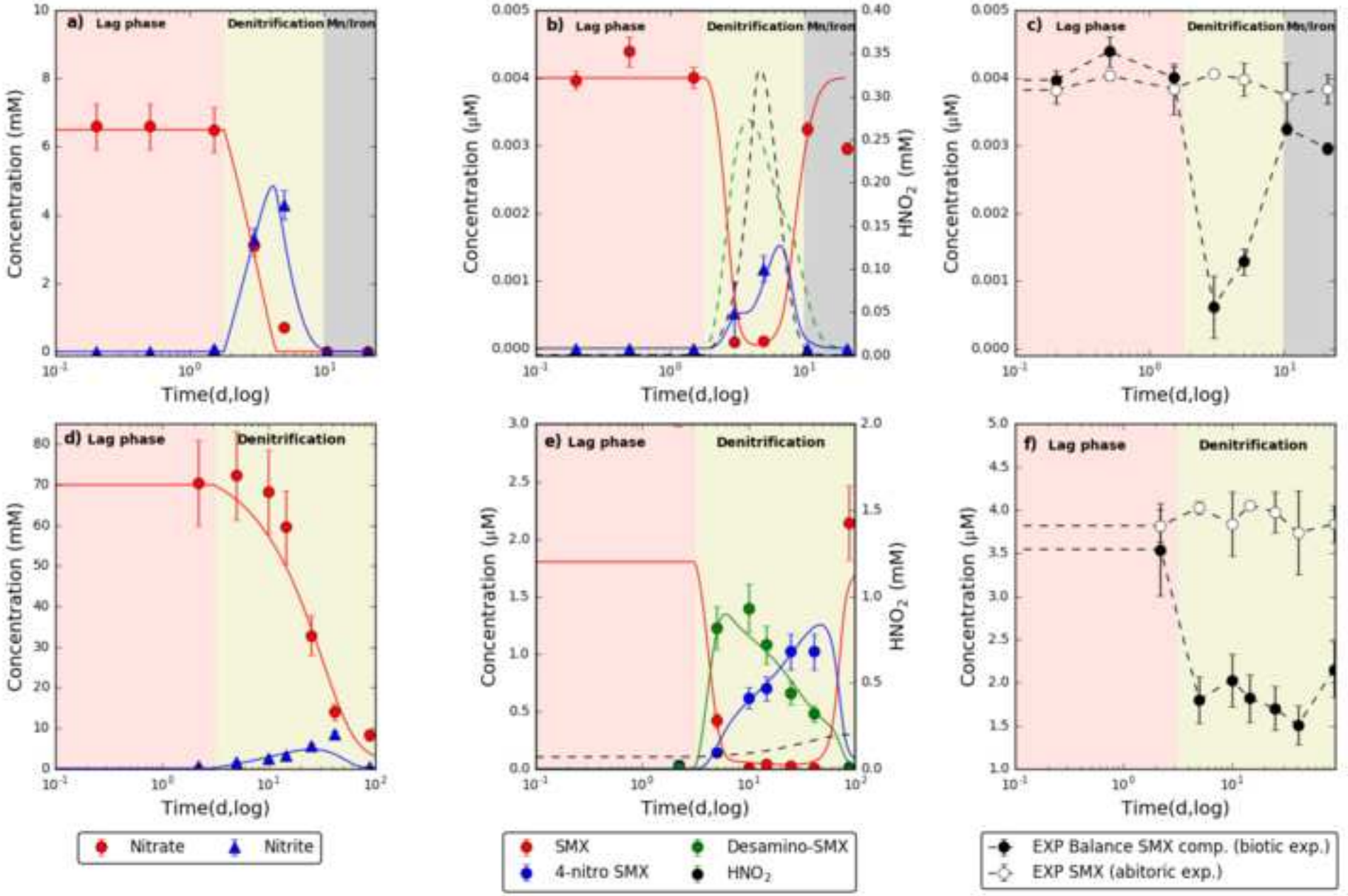

Figure3
Click here to download high resolution image

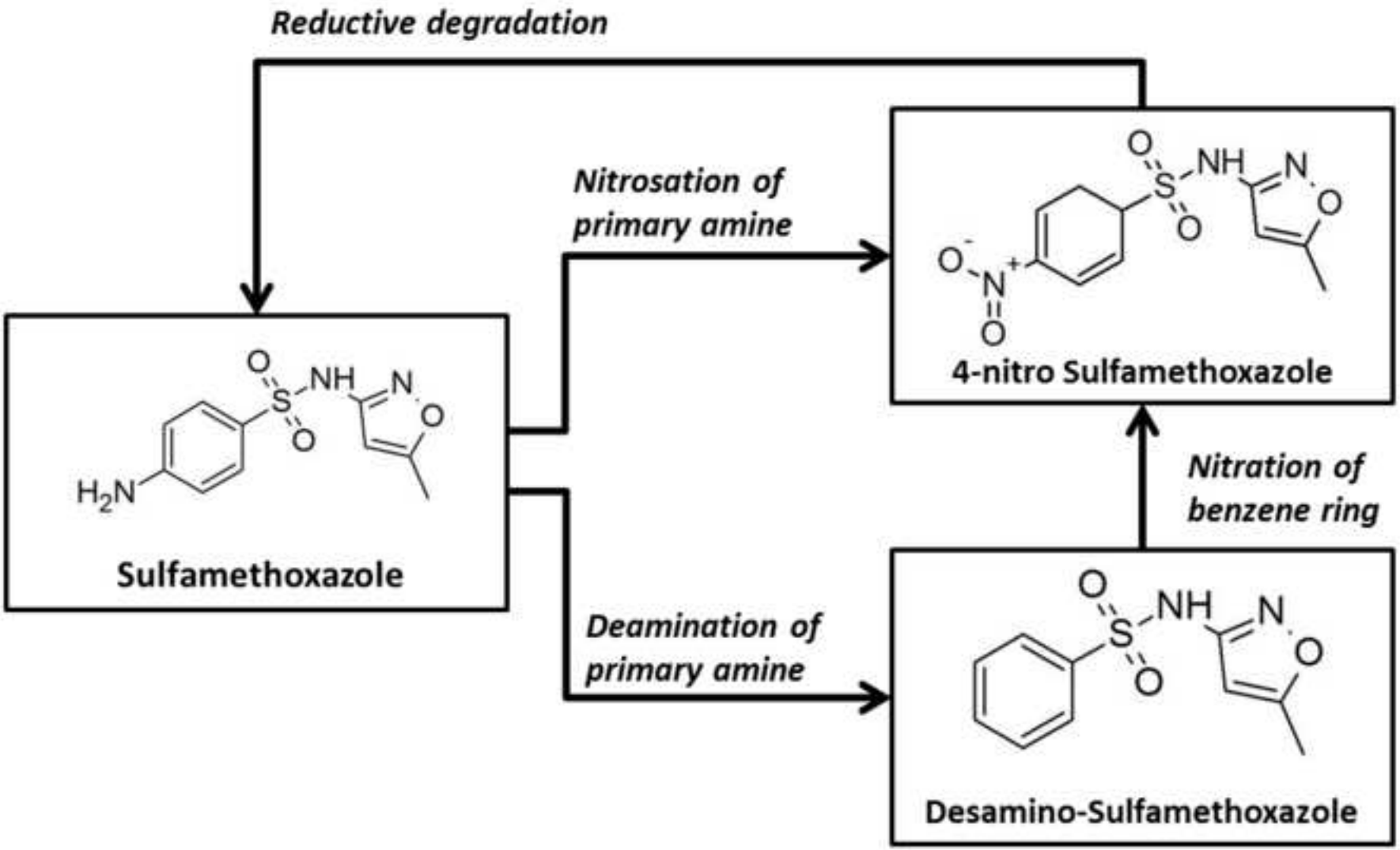

Figure4

Click here to download high resolution image

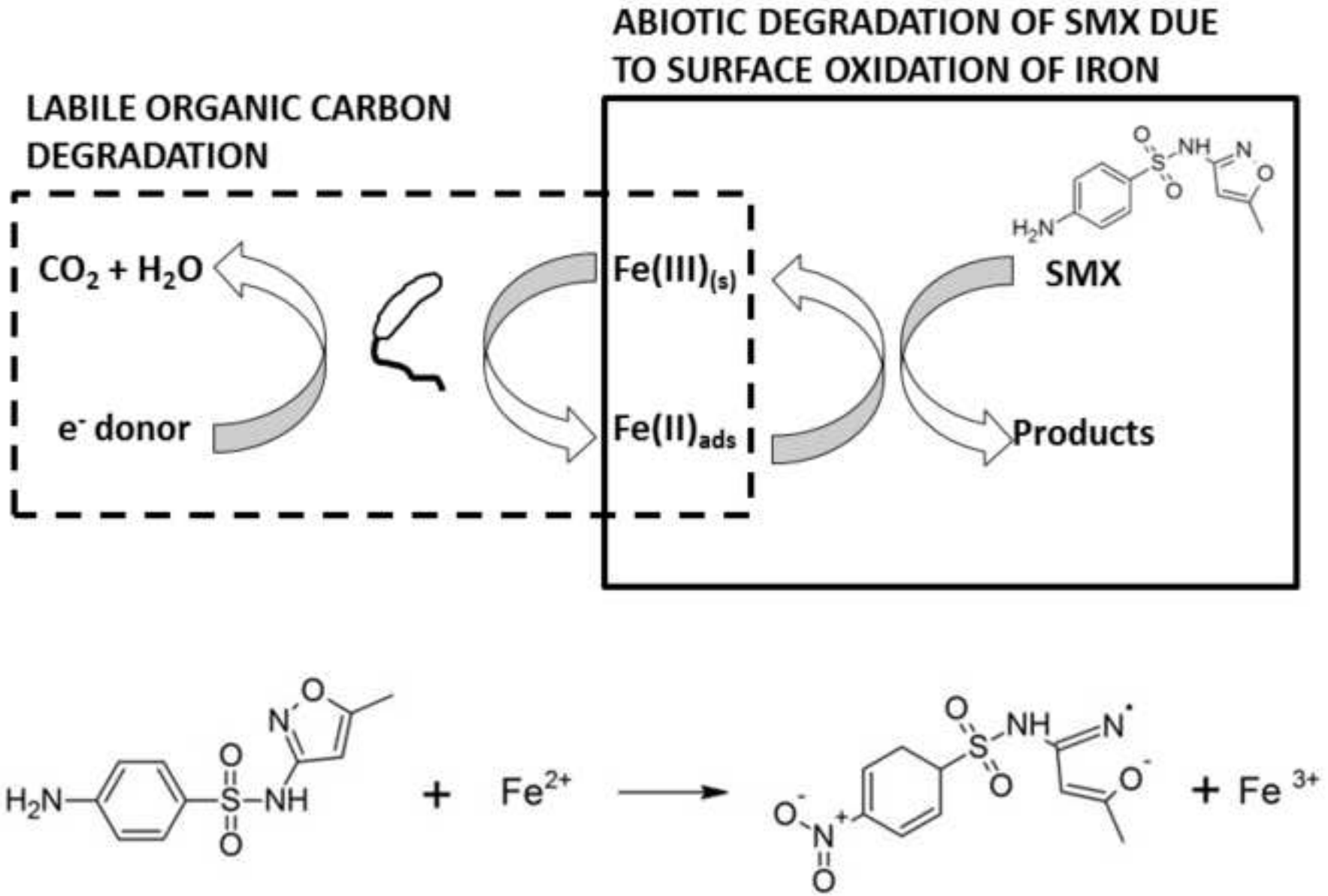

Figure5
Click here to download high resolution image

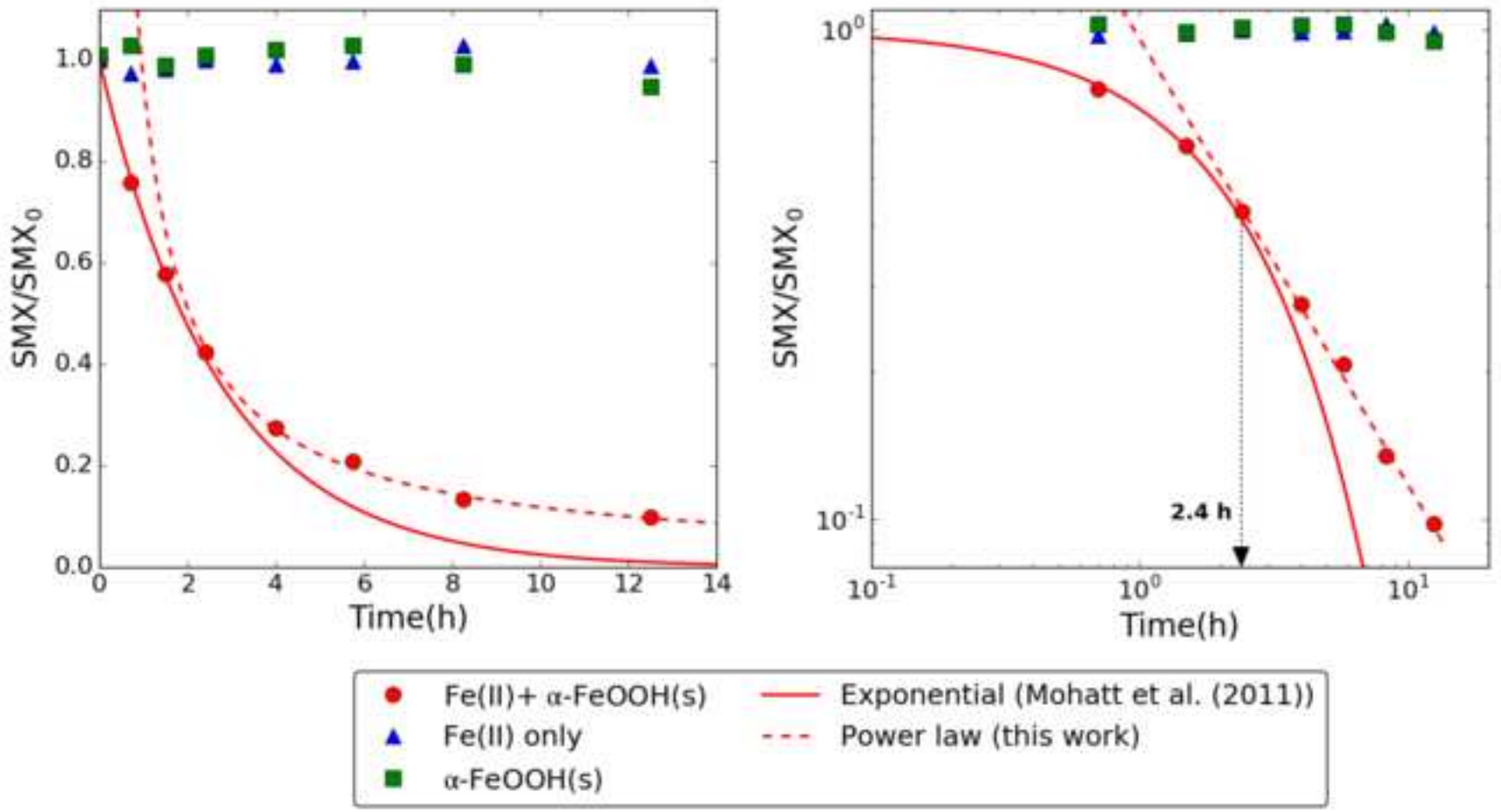

Electronic Supplementary Material (for online publication only)

Click here to download Electronic Supplementary Material (for online publication only): SMX_supporting_information_v3.docx